Lab on a Chip

Dynamic Article Links

Cite this: *Lab Chip*, 2012, **12**, 1717

www.rsc.org/loc

PAPER

Micro-patterned porous substrates for cell-based assays†

Fanny Evenou,[a] Jean-Marc Di Meglio,[a] Benoit Ladoux[ab] and Pascal Hersen*[ab]

Received 28th July 2011, Accepted 15th February 2012
DOI: 10.1039/c2lc20696j

In the search for new therapeutic chemicals, lab-on-a-chip systems have recently emerged as innovative and efficient tools for cell-based assays and high throughput screening. Here, we describe a novel, versatile and simple device for cell-based assays at the bench-top. We created spatial variations of porosity on the surface of a membrane filter by microcontact printing with a biocompatible polymer (PDMS). We called such systems Micro-Printed Membranes (μPM). Active compounds dispensed on the porous areas, where the membrane pores are not clogged by the polymer, can cross the membrane and reach cells growing on the opposite side. Only cells immediately below those porous areas could be stimulated by chemicals. We performed proof-of-principle experiments using Hoechst nuclear staining, calcein-AM cell viability assay and destabilization of the cytoskeleton organisation by cytochalasin B. Resulting fluorescent staining properly matched the drops positioning and no cross-contaminations were observed between adjacent tests. This well-less cell-based screening system is highly flexible by design and it enables multiple compounds to be tested on the same cell tissue. Only low sample volumes in the microlitre range are required. Moreover, chemicals can be delivered sequentially and removed at any time while cells can be monitored in real time. This allows the design of complex, sequential and combinatorial drug assays. μPMs appear as ideal systems for cell-based assays. We anticipate that this lab-on-chip device will be adapted for both manual and automated high content screening experiments.

Introduction

There is an increasing demand from pharmaceutical, cosmetic and biotechnology companies for reliable, cost-effective methods to evaluate the therapeutic potential of a drug candidate or the toxicity of chemicals on living systems. The European Union (EU) has initiated the REACH program (Registration, Evaluation, Authorization and Restriction of Chemical substances) which implies that an impressive number of toxicity assays will have to be performed.‡ At the same time, cosmetic-related animal testing has been banned in 2009. More generally, the EU strongly encourages refraining from using animals for testing chemicals. The European Partnership for Alternative Approaches to Animal Testing (EPAA) goal is to develop and validate alternative strategies to animal testing.§ Whereas high-throughput screening (HTS) methods enable to study the interactions between test molecules and biochemical targets, high-content screening (HCS) methods, also referred to as cell-based assays, aim at studying the effects of biochemical compounds in the context of the living cell.[1–3] HCS methods are emerging technologies that can be viewed as efficient alternatives to animal testing for probing the effects of chemicals on fundamental biological processes.

HCS assays usually combine chemical delivery multiplexing ability with a cell culture system cast into a miniaturized, versatile format. Their design is constrained by technico-economical aspects including low-cost fabrication, compatibility with existing systems (fluid dispensers, microscopy, plate readers, *etc.*) and the need to perform fast analysis. So far, several frameworks for performing cell-based assays have been proposed from the simple multi-well microplates to more sophisticated technologies such as cell microarrays. Those usually refer to highly miniaturized systems with greater screening capabilities than standard microplate-based cultures. In such systems, cells can be arrayed on a substrate using surface patterning. In particular, high-resolution printing of cell-adhesion proteins can produce high-density arrays of individual cells with standardized morphology and behaviour.[4] Substrates can alternatively be arrayed with polymers, proteins, peptides, or antibodies, and specific interactions with post-seeded cells can be analyzed.[2] To deliver drug and chemical samples at specific locations, gel-based technologies use an aqueous gel as a diffusion matrix between the chemical samples and the target cells. Compounds may be

[a]*Matière et Systèmes Complexes, UMR 7057 CNRS & Université Paris Diderot, 75013 Paris, France. E-mail: pascal.hersen@univ-paris-diderot.fr*
[b]*The MechanoBiology Institute, National University of Singapore, Singapore 117411*

† Electronic supplementary information (ESI) available: 5 figures and 1 movie. ESI-1 shows μPMs with different patterns. ESI-2 shows SEM images of MDCK cells grown on a μPM. ESI-3 shows the μPM. ESI-4 is a movie showing a time lapse of cells treated with calcein-AM. ESI-5 evidences that adjacent tests do not overlap. ESI-6 shows quantitative measurements of diffusion across a μPM. See DOI: 10.1039/c2lc20696j

‡ http://ec.europa.eu/environment/chemicals/reach/reach_intro.htm

§ http://ec.europa.eu/enterprise/epaa/index_en.htm

directly spotted onto a gel containing the cells or arrayed onto a surface subsequently assembled to a gel-based assay format.[5] More generally, microarrayed compound screening (μARCS) assays are well-less high-throughput screening assays which use a porous matrix as a diffusion interface between arrayed test samples and biochemical or biological targets. Cell-based μARCS systems involve three components: a microarrayed chemical compound sheet, a porous matrix, and cultured cells.[6,7] It has been assumed that provided the assays were carefully timed, radial diffusion within the porous matrix was slow enough to prevent overlapping of individual assays. So far, several methods derived from μARCS technology have been successfully used in studies involving mammalian cells.[7–13]

Here we present a device for cell-based assay with the ability to address *independently* and *sequentially* several chemicals to multiple groups of cells from the *same* monolayer of cells. Our method (Fig. 1) is based on the modification of a porous membrane filter by micro-contact printing of polydimethylsiloxane (PDMS). We call such substrates *Micro-Printed Membranes* (μPM). The central idea is to culture cells on the *verso* side of the μPM while chemicals can be delivered by drop deposition onto the porous areas of the *recto* side (see Fig. 1D).

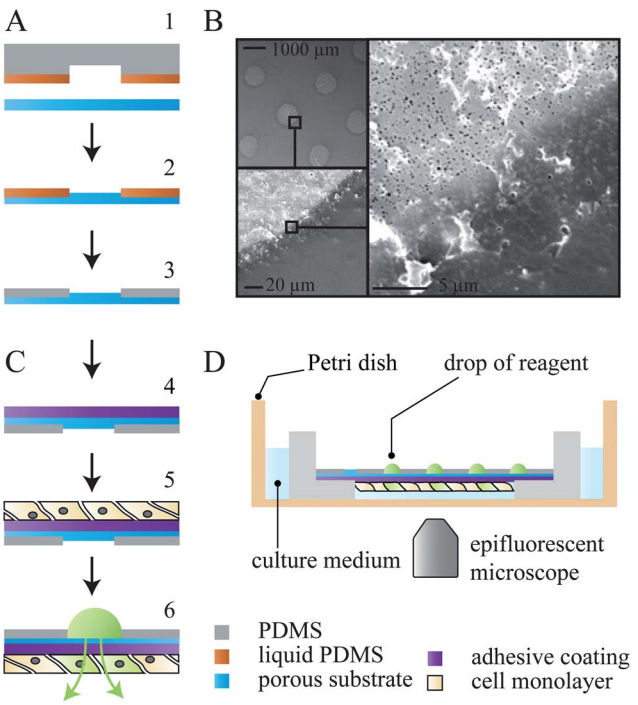

Fig. 1 Micro-Printed Membrane (μPM). (A) Fabrication steps: (1) A stamp was inked with a mix of liquid PDMS and its curing agent and used to print a membrane filter by contact printing (2), which was then heated to cure the thin layer of deposited PDMS (3). The patterned side is called the *recto* side. (B) SEM images of a μPM with an 8 × 8 array of 1 mm diameter disks. Single pores can be seen in the porous area at high magnification. (C) μPM usage. After surface coating to promote cell adhesion (4), cells were cultured (5) on the *verso* of μPMs. Droplets of chemicals placed onto porous areas on the *recto* can only affect cells locally (6). (D) A μPM with cultured cells was mounted on a stainless steel device (ESI-3†), *recto* side up. Drops of reagent were deposited at dedicated areas on the *recto* side using a micro-pipette.

Chemicals diffuse through the membrane and interact locally with cells spread underneath the porous areas (Fig. 1). Their effect on target cells can be monitored using time-lapse microscopy. Similarly to μARCS, μPMs are designed for rapid, cost-effective, benchtop fabrication. They also allow for spatially defined delivery of different compounds to groups of cells of the same culture thus reducing batch-to-batch variability and allowing to study cells within the context of cell–cell interactions, *i.e.* closer to *in vivo* conditions.

In this article, we report proof-of-principle experiments demonstrating the suitability of μPM for cell-based assays. As we will show in this article, μPMs have several practical advantages over μARCS methods. Their fabrication is easier (contact printing of PDMS followed by a curing step, see Methods) and more versatile. Indeed, any pattern of porosity can be printed (dots of various sizes, lines, squares, …, see ESI-1†) whereas conventional μARCS uses micro-arraying robots with predefined arrays of pins to perform chemical deposition.[9] More importantly, in μARCS all the compounds are applied simultaneously (sandwich configuration) and for the same duration. Here the cells are first grown to the desired state and only then the chemicals are delivered to the selected positions by drop deposition. This allows treatment of groups of cell at different times, for different durations and to apply repeated or sequential treatment.

Methods

Membrane patterning

The fabrication method of μPMs is shown in Fig. 1. Commercially available porous filter membranes were patterned with PDMS by microcontact printing. They can be produced in large quantities from a single master stamp. Briefly, a 10 : 1 mass ratio mixture of PDMS base and curing agent (Silgard 184 W C^{-1}, Dow Corning) was degassed in a vacuum chamber, poured over a silanized master wafer and then cured for several hours at 65 °C. The master wafers were prepared by soft lithography as previously described in ref. 16. The PDMS stamp was peeled off from the master, and then inked with a liquid mixture of PDMS and its curing agent which was subsequently transferred to a membrane filter by contact printing. Patterned membranes were immediately cured on a hot plate at 100 °C for 45 min. The patterned surface of the membrane is designated as the *recto* side. μPMs were bound to a ~1 mm thick PDMS ring for easy handling. The structure of the patterned membranes was analyzed by scanning electron microscopy (JEOL-JSM 6100).

The pores of the membrane were selectively clogged by the PDMS polymer, thus demarcating areas where diffusion across the membrane was allowed or not. Differences in the membrane pores between PDMS-printed and unprinted regions can be seen on SEM (Scanning Electron Microscopy) images (Fig. 1B). Different types of porous membranes were successfully printed including polycarbonate, polyester and alumina membranes. In this study we mainly used Isopore membrane filters purchased from Millipore. They are polycarbonate filter membranes manufactured using track-etching technology. Unless noted otherwise, the membranes were 25 mm in diameter, with an average porosity of 13.8% and pores of 0.22 μm in diameter. They could

be patterned with various shapes over a broad range of sizes (see ESI-1†). When stamping with an array of 1 mm diameter holes, μPMs with an array of porous disks were obtained. The diameter of the porous disks was smaller than expected, with an average diameter of 0.90 ± 0.04 mm. This was due to a slight overflow of the thin, uncured, liquid PDMS at the surface of the membrane before its reticulation was complete. For the same reason, the finest details that could be printed by our manual method were as low as 0.1 mm wide lines, but those small features were not very reproducible (see ESI-1†). To ensure a high reproducibility of the patterns, it was best to use patterns no smaller than typically 1 mm. Yet, the ~1 mm porous disks were almost twice smaller than the wells of conventional 1536-well microplates which are 1.63 mm wide. This ensures that μPM can have high density arrays of porous regions and thus are compatible with high-throughput applications. Decreasing further the size of the porous area is not advisable for maintaining a sufficiently large sample of treated cells as well as to ensure easy drop delivery.

Cell culture on patterned membranes

MDCK (Madin-Darby Canine Kidney) adincells are highly proliferative cells which tend to organize themselves into a cellular monolayer under conventional tissue culture conditions. Since μPMs are not transparent, we used a fluorescently labeled cell-line stably expressing RFP-actinin. Cells were routinely cultured in 25 cm^2 tissue culture flasks (TPP), in a 37 °C incubator with 5% CO_2/95% air. Culture medium was Dulbecco's Modified Eagle Medium (DMEM; PAA) supplemented with 10% fetal bovine serum (FBS; PAA), 100 units per mL penicillin and streptomycin (Gibco) and 100 μg mL^{-1} kanamycin (Sigma). μPMs were sterilized on both sides by UV treatment for a total of 50 min, rinsed with phosphate buffered saline (PBS; PAA), then the membrane *verso* side was coated with 0.3 g L^{-1} type I collagen (Gibco) for about two hours at room temperature and rinsed once with water and twice with PBS. MDCK cells were cultured on the collagen-coated *verso* side of the μPMs in a 37 °C incubator and were allowed to grow to near confluence (two or three days) before the assay starts.

Biological assays

Hoechst 33342 (H3570) and calcein-AM (C1430) were purchased from Invitrogen. MDCK cells were cultured on the *verso* side of a μPM. Near-confluent cell cultures were rinsed once with culture medium then mounted on a stainless steel device (see ESI-3†) in a 35 mm dish, with *recto* side up and cultured cells on the *verso* side immersed in 4 mL of culture medium. Alternate and successive deposition of Hoechst (4 μg mL^{-1}) and calcein-AM (5 μM) were performed on the same μPM. 1 μL drops were deposited onto porous areas on the *recto*, the cultures were incubated for 40 min at 37 °C, then the *recto* side was rinsed twice with culture medium before imaging. In the case of successive assays at the same location, the first deposited drops were aspirated with a micropipette and the porous disks were rinsed twice with drops of culture medium before performing the next drop deposition. After treatments, cell cultures were observed using fluorescence microscopy (Olympus BX51WI). Cytochalasin B (CB) was purchased from Sigma. 1.5 μL drops of 5 μg mL^{-1} CB were deposited onto porous disks and the drug was allowed to diffuse for 20 min. Cells were imaged by time-lapse fluorescence microscopy using an inverted fluorescence microscope (Olympus IX71).

Results

We first assessed the possibility to deliver simultaneously the same compound at specific locations on a monolayer of MDCK cells. We used μPMs patterned with an 8×8 array of 1 mm diameter porous disks, 1 mm distant from each other. Note that polycarbonate membranes are hydrophilic and PDMS is hydrophobic. This was very practical since drops of aqueous solutions did not spread over the μPM *recto* but remained confined in the porous regions which are surrounded by a very thin layer of PDMS. Therefore, adjacent drops of a few microlitres remained isolated and did not mix. MDCK cells were cultured on the *verso* of a collagen-coated μPM. They grew to near confluence, forming after a few days, a continuous cell monolayer spreading over the entire surface of the membrane (Fig. 2 and ESI-2†). Then the μPM was mounted on a stainless steel device (see ESI-3†) *recto* side up. The cells on the *verso* were bathed in 4 mL of culture medium. A 1 mL drop of 2 μM calcein-AM was spread over the *recto* so as to cover the entire surface of the μPM. In living cells, the intracellular calcein-AM is hydrolyzed into green fluorescent calcein. Here, a green fluorescence signal was detected after 10 min inside the porous disks only and progressively increased over time (see Fig. 3A and B and ESI-4†). After one hour of treatment, calcein green fluorescence was primarily detected inside the patterns. Outside, the fluorescence level was very low and did not show an increase with time at the level of single cells (Fig. 3B), though the background level progressively increased as excess calcein-AM diluted in the

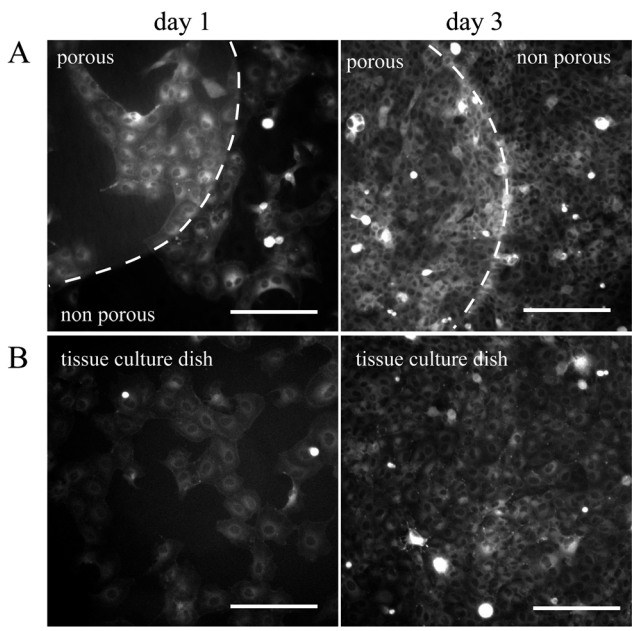

Fig. 2 Morphology of MDCK cells expressing actinin-RFP cultured (A) on a collagen-coated *verso* side of a μPM and (B) on a tissue culture treated dish. Pictures were taken one day post-seeding and at confluence (day 3). Scale bar is 200 μm. The dashed line indicates the border of a 1 mm porous disk.

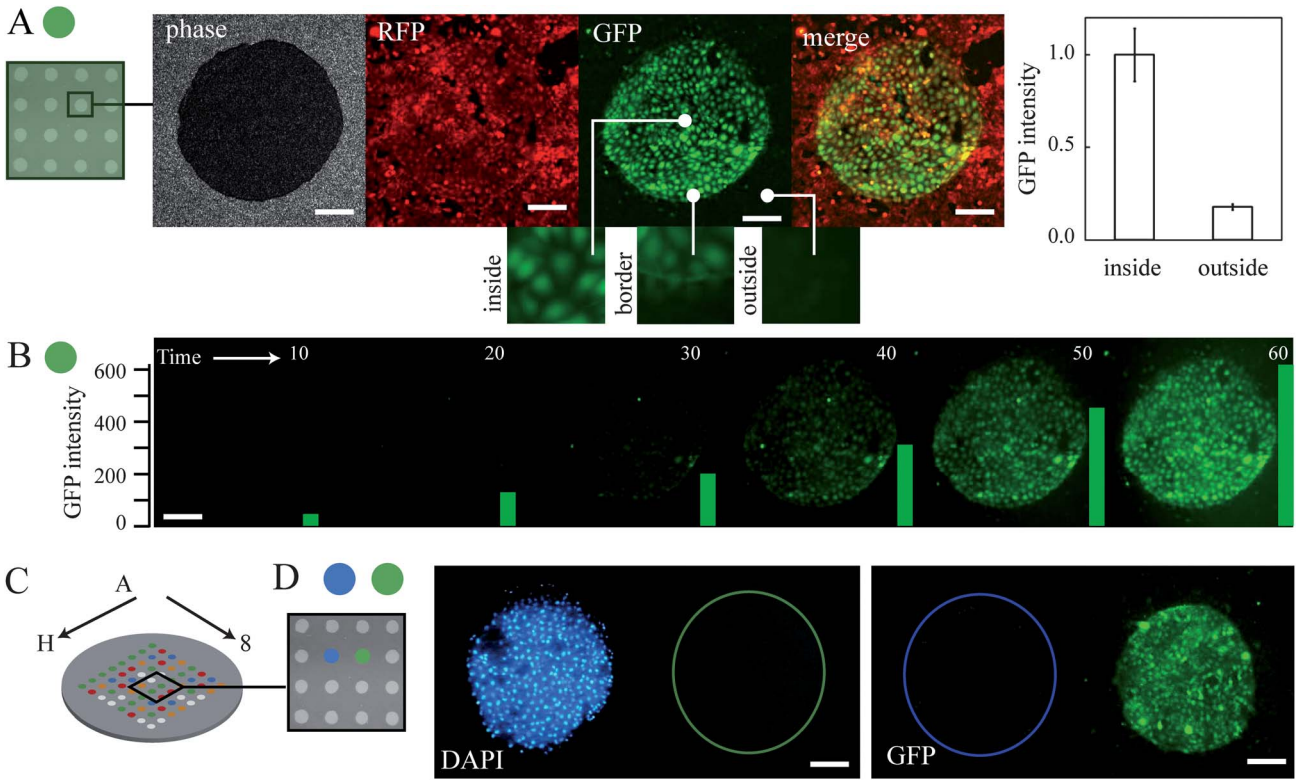

Fig. 3 Diffusion assays. (A and B) Calcein-AM assay: 1 mL drop of calcein-AM solution was spread over the *recto* side of a μPM with an 8 × 8 array of 1 mm diameter disks and with MDCK cells cultured on the *verso* side. (A) Phase contrast, RFP and GFP images showing, respectively, the porous disk, the monolayer of cells and the green fluorescent calcein staining after 1 hour diffusion. The graph on the right represents the average intracellular fluorescence intensity after 1 hour ($N = 11$ disks, fluorescence was measured using ImageJ[14]). (B) Time-lapse fluorescence imaging of intracellular calcein-AM hydrolysis into green fluorescent calcein over 1 hour (see also ESI-4†). The background fluorescence intensity also increased over time as calcein-AM diluted and got hydrolyzed in the culture medium. The green bars indicate the increase of the fluorescence signal inside the porous area relatively to the background. (C) Sketch of a μPM with an 8 × 8 array depicting the idea of semi high-throughput drug assays. (D) Hoechst nuclear staining (seen using DAPI filters) and calcein-AM cell viability assay (seen using GFP filters) were simultaneously performed on the same μPM. 1 μL drops of each reagent were deposited in adjacent disks. No cross-contamination was observed between the different assays. Scale bars indicate 200 μm.

culture medium where it was partly hydrolyzed by serum esterases. This experiment showed that calcein-AM was mainly captured and hydrolyzed by the cells located below the patterns *i.e.* below the porous regions of the μPM (Fig. 3A and ESI-5†).

Next, we tested the possibility to deliver different chemicals at defined locations of the same cell culture. Microlitre drops of either Hoechst or calcein-AM were deposited on the same μPM onto adjacent disks separated by ~1 mm. Green and blue fluorescences characteristic of intracellular calcein and Hoechst nuclear staining, respectively, were selectively observed (Fig. 3C and D). Moreover, there was no cross-contamination (Fig. 3D). This demonstrated the possibility to conduct several, distinct assays on different regions of the same monolayer of cells using a μPM.

Importantly, using μPM allows for transient and repeated biochemical assays at the same location. Indeed, reagent drops can be removed and replaced at any time using a micro-pipette. Obviously, droplet dispensers may conveniently be used to automate this process. Here again, we used Hoechst and calcein-AM for demonstration. The two dyes, Hoechst first, were successively deposited at the same location on the *recto* side and were incubated for 40 min each. Using this sequential delivery, cells below the porous regions were successfully stained with both dyes (Fig. 4A).

The previous examples were based on monitoring a change in the fluorescence level of groups of cells locally stimulated by a chemical compound or a fluorescent dye. In a final set of experiments, cytochalasin B was used to demonstrate that it is also possible to observe other output such as changes in the organization of a cell cytoskeleton. CB is known for inhibiting actin polymerization and thus to strongly disrupt the cytoskeleton organization.[15] Time-lapse fluorescence imaging of MDCK cells expressing actinin-RFP grown on a μPM and subjected to treatment with CB showed that the cells below the porous disks were very quickly affected by the drug. Cells contracted and actinin appeared to both concentrate within the center of the cells and to exhibit a punctuate peripheral staining (Fig. 4B). Cells at the periphery of the disks appeared affected by the drug to a lesser extent and no effect could be observed beyond ~80 μm (Fig. 4B).

Taken together, we have demonstrated that μPMs can be used to perform complex chemical assays on a monolayer of MDCK cells. Other cell types can be assayed too. For instance, 3T3 fibroblasts were cultured on μPMs coated with fibronectin and

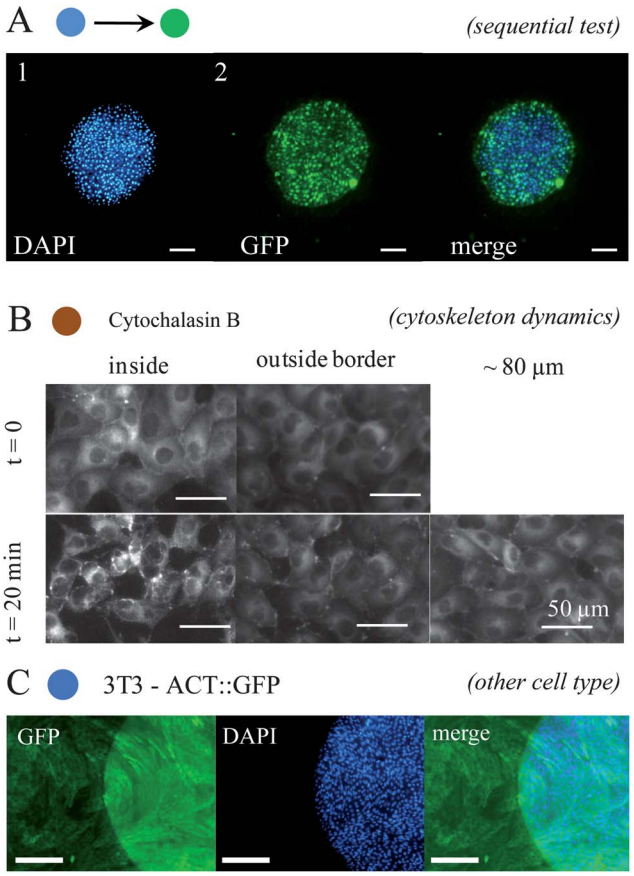

Fig. 4 Sequential test can be done with µPM. (A) Sequential assays. Hoechst (DAPI) and calcein-AM (GFP) were sequentially deposited at the same location by successive drop depositions. Scale bars are 200 µm. (B) Cytoskeleton reorganization. A drop of cytochalasin B was placed on top of a porous disk of a µPM for 20 min. Below the porous disk cells, which are expressing actinin-RFP, displayed a change in cell shape, cell–cell contact and actinin-RFP distribution, whereas peripheral cells exhibited only slight changes in their morphology. No effect of the CB was observed beyond typically 80 µm from the porous disk periphery. (C) 3T3 fibroblasts expressing actin-GFP were cultured on a µPM and their nuclei were locally stained with Hoechst by diffusion through the membrane. Scale bars are 200 µm.

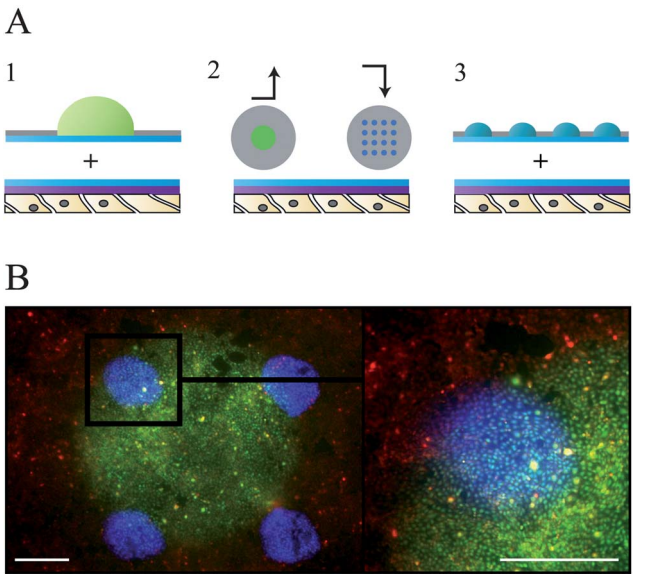

Fig. 5 Stackable µPMs. (A) MDCK cells were cultured on a non-patterned membrane with 0.22 µm pore diameter. (1) A µPM was applied on its back side and then calcein-AM was deposited on the porous disk. (2) The µPM was replaced by one with a different porous pattern. (3) 2 µL drops of Hoechst were deposited on porous disks of the new µPM. (B) Overlay of RFP (cells), GFP (calcein) and DAPI (nuclei). Scale bars are ~1 mm.

diffusion assays were successfully performed using Hoechst nuclear staining (Fig. 4C).

Finally, we tested if µPM devices could be extended into a more versatile system using stackable configurations (Fig. 5). We cultured MDCK cells on the collagen-coated side of a *non-patterned* membrane. This membrane filter was then placed into the µPM holder (Fig. 1 and ESI-3†), and a µPM with a single 3 mm diameter porous disk was placed on top of it. Calcein-AM was deposited on the *recto* side, crossed both membranes and reached the cells on the *verso* of the non-patterened membrane. Note that it was better to use a µPM with larger pores of 0.8 µm to avoid slowing down the chemical delivery through the two stacked membrane filters. After 30 min incubation, we replaced the top µPM by a different µPM patterned with an array of 1 mm porous disks. Hoechst drops were added onto the porous areas of the *recto* side. The dye successfully stained the nucleus of the targeted cells (Fig. 5). This way we obtained groups of neighbouring cells stimulated by either calcein-AM, Hoechst, both chemicals, or none of them on the same epithelium. Hence, the stackable µPMs method allows designing of complex cell-based assays where the patterns of chemical delivery can be changed with both time and space.

Conclusion

We developed an original and versatile well-less technology for performing cell-based assays. It combines on the same substrate, the target monolayer of cells on one side and an array of porous regions for drop delivery on the other side. Using calcein-AM cell viability assay, Hoechst nuclear staining and cytochalasin B, we demonstrated that different biological assays can be simultaneously performed on the same cell culture without cross-contamination between neighbouring assays. Moreover, different drugs could be successively assayed at the same tissue location. Such a well-less and flexible cell-based assay appears suitable for assessing the effects of different compounds applied separately or sequentially and can be easily adapted for the design of combinatorial assays.

Being able to perform transient, sequential or repeated drug treatment is the most important advantage of our system compared to conventional µARCS. Among several potential applications, one can mention the importance of assaying cell recovery from short exposure to drugs. Modeling the timescales of adaptation and recovery to inhibitors is indeed required to better understand their mode of action. This is for example the case for drugs affecting the cytoskeleton integrity, such as the cytochalasin we used here, which effects duration could be measured using µPMs. Another important application would be

to use our system to perform repeated dose toxicity of drugs on mammalian cells. Such toxicity tests are now required for most cosmetics and chemicals and cannot be performed with μARCS. Finally, sequential drug delivery can open the way to the study of synergetic and agonistic effects between drugs. As an example, the apoptotic inducer TRAIL (TNF-related apoptosis-inducing ligand) has been shown to be more or less effective depending on the presence of various additives.[17,18] Using our system would allow sequential treatment of cells with combination of additives and TRAIL and thus to screen for TRAIL apoptotic enhancers in both sequential and simultaneous dosing modalities as done in ref. 19.

Finally, as for μARCS, attention should be paid on the fact that the precision of chemical delivery in space is limited by experimental parameters, notably chemical concentration and treatment duration. With time, chemicals would diffuse away from the porous patterns thus potentially affecting cells located further away from the chemical source. However, this effect is limited by the dilution of the test compounds into the culture medium (see ESI-6†). To prevent assays from overlapping, different parameters such as the concentration of the test compounds, the experiment duration (drops can be removed at any time), the porosity of the membrane filter, and the distance between neighbouring assays have to be carefully chosen.

Here, we described a new method that can transform a monolayer of cells into the equivalent of a high density array plate for screening. Although we focused on conducting proof-of-principle experiments, our approach can be readily used at the benchtop. We proposed that μPMs are ideal candidates for HCS applications and that high-throughput systems can be designed based on this approach. In particular, its integration into a microfluidic device could lead to fast and reliable sequential drug delivery, although at the cost of complexity. Importantly, we anticipate that single and stackable μPMs will allow quick, customized and inexpensive semi high-throughput cell-based screening assays to be performed routinely at the bench.

Acknowledgements

MDCK cells were kindly provided by W.J. Nelson (Stanford, USA). 3T3 fibroblasts were kindly supplied by Dr M. Coppey (Institut Jacques Monod, Paris). We wish to thank Nils Gauthier for his critical reading of this manuscript. PH is supported by an ANR Jeunes Chercheurs and the program C'Nano IDF. FE is supported by a CNRS postdoctoral fellowship.

Notes and references

1 D. L. Taylor, E. S. Woo and K. A. Giuliano, *Curr. Opin. Biotechnol.*, 2001, **12**, 75–81.
2 D. Castel, A. Pitaval, M.-A. Debily and X. Gidrol, *Drug Discovery Today*, 2006, **11**, 616–622.
3 T. G. Fernandes, M. M. Diogo, D. S. Clark, J. S. Dordick and J. M. Cabral, *Trends Biotechnol.*, 2009, **27**, 342–349.
4 M. Thery, V. Racine, M. Piel, A. Pepin, A. Dimitrov, Y. Chen, J. B. Sibarita and M. Bornens, *Proc. Natl. Acad. Sci. U. S. A.*, 2006, **103**, 19771–19776.
5 M. Hoever and P. Zbinden, *Drug Discovery Today*, 2004, **9**, 358–365.
6 B. A. Beutel, M. E. Schurdak, M. J. Voorbach, D. J. Burns and M. K. Joseph, *US Pat.*, 5976813, 1999.
7 M. E. Schurdak, M. J. Voorbach, L. Gao, X. Cheng, X. H. Chung, K. M. Comess, S. M. Rottinghaus, U. Warrior, H. N. Truong, D. J. Burns and B. A. Beutel, *J. Biomol. Screening*, 2001, **6**, 313–323.
8 S. M. Gopalakrishnan, R. B. Moreland, J. L. Kofron, R. J. Helfrich, E. Gubbins, J. McGowen, J. N. Masters, D. Donnelly-Roberts, J. D. Brioni, D. J. Burnsand and U. Warrior, *Anal. Biochem.*, 2003, **321**, 192–201.
9 S. N. Bailey, D. M. Sabatini and B. R. Stockwell, *Proc. Natl. Acad. Sci. U. S. A.*, 2004, **101**, 16144–16149.
10 M. Y. Lee, C. B. Park, J. S. Dordick and D. S. Clark, *Proc. Natl. Acad. Sci. U. S. A.*, 2005, **102**, 983–987.
11 M. Y. Lee, R. A. Kumar, S. M. Sukumaran, M. G. Hogg, D. S. Clark and J. S. Dordick, *Proc. Natl. Acad. Sci. U. S. A.*, 2008, **105**, 59–63.
12 J. Wu, I. Wheeldon, Y. Guo, T. Lu, Y. Du, B. Wang, J. He, Y. Hu and A. Khademhosseini, *Biomaterials*, 2011, **32**, 841–848.
13 H. Tavana, A. Jovic, B. Mosadegh, Q. Y. Lee, X. Liu, K. E. Luker, G. D. Luker, S. J. Weiss and S. Takayama, *Nat. Mater.*, 2009, **8**, 736–741.
14 W. S. Rasband, *ImageJ*, U. S. National Institutes of Health, Bethesda, Maryland, USA, 1997–2011, http://imagej.nih.gov/ij/.
15 S. MacLean-Fletcher and T. D. Pollard, *Cell*, 1980, **20**, 329–341.
16 Y. Xia and G. M. Whitesides, Soft lithography, *Annu. Rev. Mater. Sci.*, 1998, **28**, 153–184.
17 Y. Mizutani, H. Nakanishi, O. Yoshida, M. Fukushima, B. Bonavida and T. Miki, *Eur. J. Cancer*, 2002, **38**, 167–176.
18 B. Gliniak and T. Le, *Cancer Res.*, 1999, **59**, 6153–6158.
19 D. J. Taylor, C. E. Parsons, H. Han, A. Jayaraman and K. Rege, *BMC Cancer*, 2011, **11**, 470.

